MODELING THE TRAJECTORY TRACKING ACCURACY OF AN AUTONOMOUS CATAMARAN PATROL VESSEL UNDER DIFFERENT POSITIONAL DATA DISTURBANCE CONDITIONS

ANDRES UDAL
Tallinn University of Technology, School of Information Technologies, Department of Software Science, Tallinn 16812, Akadeemia tee 15a, Estonia
e-mail: andres.udal@taltech.ee
Orcid: 0000-0002-8465-6757

JAANUS KAUGERAND
Tallinn University of Technology, School of Information Technologies, Department of Software Science, Tallinn 16812, Akadeemia tee 15a, Estonia
e-mail: jaanus.kaugerand@taltech.ee
Orcid: 0000-0001-8678-0295

HEIGO MÕLDER
Tallinn University of Technology, School of Engineering, Department of Electrical Power Engineering and Mechatronics, Tallinn 19086, Ehitajate tee 5, Estonia
e-mail: heigo.molder@taltech.ee
Orcid: 0000-0002-6399-7018

IGOR ASTROV
Tallinn University of Technology, School of Information Technologies, Department of Software Science, Tallinn 16812, Akadeemia tee 15a, Estonia
e-mail: igor.astrov@taltech.ee
Orcid: 0000-0003-0761-2045

SANJA BAUK
Tallinn University of Technology, Estonian Maritime Academy, Centre of Maritime Cybersecurity, Tallinn 11712, Kopli 101, Estonia
e-mails: sanja.bauk@taltech.ee; bsanjaster@gmail.com
Orcid: 0000-0003-2882-1321

ACKNOWLEDGMENTS

Research for this publication was funded by the EU Horizon2020 project MariCybERA (Agreement No. 952360).

Keywords

Autonomous vessel, cyber-risks, model-based navigation, non-GPS navigation, trajectory tracking

Abstract

A sharp increase in the importance of autonomous vehicles can be foreseen in future maritime transport. One important area of application of autonomous waterborne vehicles is the monitoring of the safety of sea routes and sea areas. In this case, an important subtask is following the desired coordinates and movement trajectories as accurately as possible, despite natural disturbances and malicious cyberattacks.

In this work, we discuss the model-based ship navigation with increased disturbance resistance to assure the desired control of a catamaran robot ship in different conditions of natural disturbances and missing global positioning data due to possible cyber-attacks. The considered example autonomous surface vessel (ASV) is a catamaran ship of 2.5 m length, developed at Tallinn University of Technology. Different from the previous studies, in this work we have completed the hydromechanical ship model with wind force model in order to simulate the influence of nonlinear environment conditions to the accuracy of ship navigation. The main result, illustrated by detailed numerical calculations, is that the availability of an accurate mathematical model of ASV together with accurate data from local sensors (in particular ship direction and wind speed sensors) can compensate for the lack of a GPS signal under cyber-attack conditions. In addition, we demonstrate with a numerical simulation how data fusion methodology, supplementing the wind effect measurements with local ship sensor data, can achieve even better navigation accuracy.

1 INTRODUCTION

Modern Information Technology (IT) and Operational Technology (OT) systems are both critical in the maritime business and industry. The IT mainly manages administrative operations, while OT includes a wide range of programable controllers, which enable the convergence of the cyber and physical systems [1;2]. Both IT and OT are vulnerable to getting cyber-attacked. Therefore, the Estonian Maritime Academy researchers work together with network security, software engineering, forensics, and human factor cyber experts to develop a holistic approach to security, safety, and resilience of maritime infrastructure. The team is working to develop methods for the early detection and prevention of system failures, whether accidental or intentional. The focus is on systems that are essential for maritime navigation, first and foremost on board the ship.

In marine navigation, Global Positioning System (GPS) as one of the Global Navigation Satellite Systems (GNSS), including Automatic Identification System (AIS), are most frequently exposed to cyber-attacks. One way to replace the loss of positioning information in the conditions of a cyber-attack, when it is necessary to steer the ship on a given course, is to rely on secure local sensors located on the ship and mathematical model of the ship and its surrounding environment. It may be estimated that the presence of an accurate model for both the ship and natural influences such as wind or currents should basically allow the ship to be navigated even in situations where global positioning information is not available. In present study we investigate relevant possibilities of recovering of the loss of global positioning information on the basis of modeling and simulation of course tracking tasks of a real catamaran Autonomous Surface Vessel (ASV) of 2.5 m length and 200 kg weight class, developed at Tallinn University of Technology [3;4].

2 A SHORT INTRODUCTION TO MARITIME CYBER THREATS

2.1 Examples of attacks against the global positioning systems

Let us assume that the GPS receiver on board is not working properly. This can happen for several reasons. For instance, the cable between the antenna and the GPS receiver may be damaged or improperly plugged in, or the receiver has inadvertently failed. However, we should be aware that GPS receiver can also be vulnerable to various types of malicious cyber-attacks such as jamming and spoofing [5].

Jamming is usually based on a small transmitter that works on almost the same frequency as the satellites. This noise can knock out the receiver in radius of several tens of miles. Jamming resistance can be increased with the Controlled Reception Pattern Antenna (CRPA) [6], but it is rather expensive and mainly available for military use. Some GPS receivers have additional capacities based on Machine Learning (ML) and Artificial Intelligence (AI) to filter out jamming signal and recover the original one [7].

Spoofing is another, more sophisticated method of disturbance. In such a case, an emitter transmits signals, which the GPS receiver will be able to read as a satellite and thereby use as a completely erroneous line of position. Spoofing will be able to cause great errors in all receivers within range of vision. It requires more complicated equipment and more competence in comparison to anti-jamming. Furthermore, it can easily be confused with multipath by the receiver, and therefore difficult to identify as an external source of error.

To avoid the negative effects of jamming and spoofing, some alternative solutions can be used like *hybrid receivers*, composed of the USA GPS, Russian Глобальная Навигационная Спутниковая Система (GLONASS), Chineze BeiDou, European Galileo, or one of two regional satellite navigation systems like Indian Regional National Satellite system (IRNSS) and Japan's Quasi Zenith Satellite System (QZSS). More precisely, when high accuracy is required, special GNSS receivers are used that can track, for instance, both GPS and GLONASS satellites simultaneously and switch from one system to the other depending on the availability and position accuracy of the satellites in the constellation. Such a system like Seatex DPS-232 developed by Kongsberg continuously receives corrections (Fig. 1). On the display, it is possible to show a plot of where the satellites are placed. Also, it is possible to get information on the signal strength and status, as well as on satellite potential deactivation. This advanced GNSS receiver has a function, which simulates the satellites' geometry Horizontal Dilution of Precision (HDOP) ahead in time for two weeks. The system includes the European Geostationary Navigation Overlay (EGNOS), which is satellite-based augmentation system with three geostationary satellites and an interconnected ground network of about forty positioning stations and two mission control centres [8]. This advanced GNSS receiver has also an extra antenna for receiving International Association of Marine Aids to Navigation and Lighthouse Authorities (IALA) corrections. The system is connected with Gyro and it has MS Windows external interface, including Dynamic Positioning (DP) one if the receiver is used for demanding offshore operations.

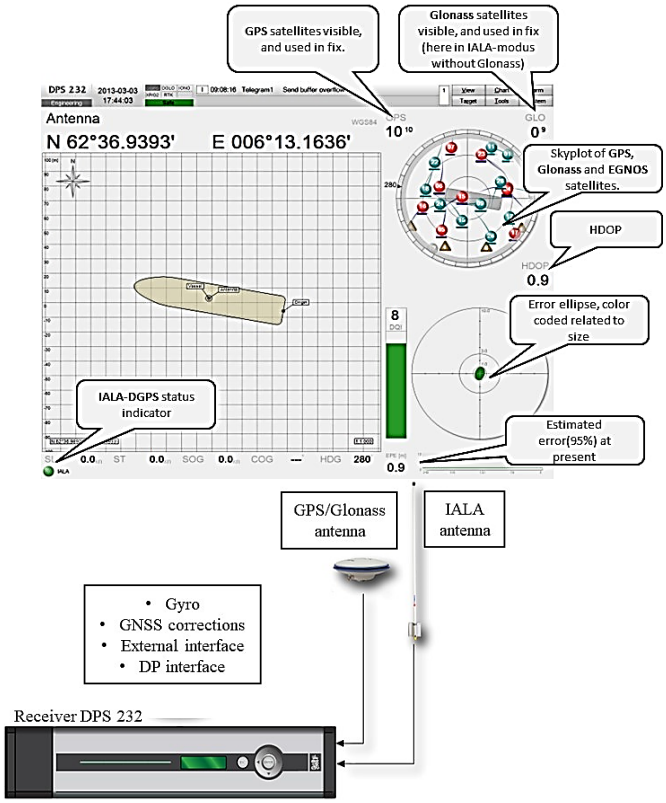

Fig. 1 Explanation of an advanced hybrid GPS and GLONASS receiver (adapted from [6]).

Other systems and devices that can support GNSS functionality are augmentation-smart support systems, stable clocks in the receivers, micro electromechanical sensors, and of course, radio, and inertial navigation, which will be in the focus of our further study. Some of these solutions are costly, but where satellite systems are used in especially critical operations, they are worth considering. To support navigational safety and security, a modernized radio-hyperbolic system such as Enhanced Loran (e-Loran) can be used, as well. Furthermore, for military purposes, a highly accurate military positioning, velocity, and timing service broadcasted is available in the form of coded Precise Positioning Service (PPS) in GPS, with accuracy of 15 m (95%) or higher. The PPS includes cryptographic keys, which remove the effects of selective availability and

spoofing, but are not available to commercial GPS users.

2.2 Recognizing and avoiding GPS and AIS cyber-attacks

In here presented example, the GPS spoofing caused a single vessel to deviate off course. In the next iteration, multiple vessels were at the same place, while they were actually tens of miles away. Namely, the master of the Atria tanker off the port Novorossiysk, reported that his GPS showed the ship to be twenty nautical miles away, close to the Gelendzhik Airport, on shore. The illustration of this situation is given in Fig. 2. The ship's real position was 44°14.0002N; 37°43.0002E, but GPS showed 44°34.6582N; 38°00.6482E. Sometime later, navigation systems at least twenty nearby ships showed all to be at the same location on the land side. Therefore, the Closest Point of Approach (CPA) alarms on many vessels announced imminent collision, which were, of course, fake alarms [9;10]. This is a very dangerous situation that requires a double check of the position and the use of all available means other than GPS to fix the position.

It is worth mentioning that the difference between the fixed position and the real one can occur if the datum on the GPS receiver and the electronic chart on Electronic Chart Display and Information System (ECDIS) are not the same. Such an error is usually 200-300 m [6]. In extreme cases, it can be several, but not twenty nautical miles, as in the case of GPS spoofing presented above, reported by the captain of the tanker Atria in the Black Sea in June 2017, and twenty other vessels sailing in the same region.

Besides jamming or spoofing GPS, there is also a risk of intentionally disabling AIS devices or hacking AIS targets. The AIS is used to identify and locate own and other ships, as well as for communication and sharing routes between ships and between ship and the shore control centre, which can support collision avoidance. Virtual AIS is used as an Aid to Navigation (AtoN) to check whether the system works as intended or not, and/or to replace virtually other aids to navigation like buoys for instance. If this system does not work properly, the radar, advanced camera systems combined with radar, double check of updated electronic charts, or a sharp lookout (in case of manned vessels) can come to the rescue.

Fig. 2 The Atria tanker GPS spoofing event (adapted from [9;10])

There are numerous vulnerabilities of AIS, since it appears in the early days of the Internet commercialisation. The most common are the lack of geographic validation, the lack of timestamp information, the lack of message authentication, and the lack of message integrity (for example, a fishing boat can pose as a different type of vessel) [5;10]. In Fig. 3 is presented a very dangerous case of AIS misuse. Fake AIS AtoNs represent green boys that can lead to the wrong, 'the 2nd channel', which is in fact shallow and no navigable waterway.

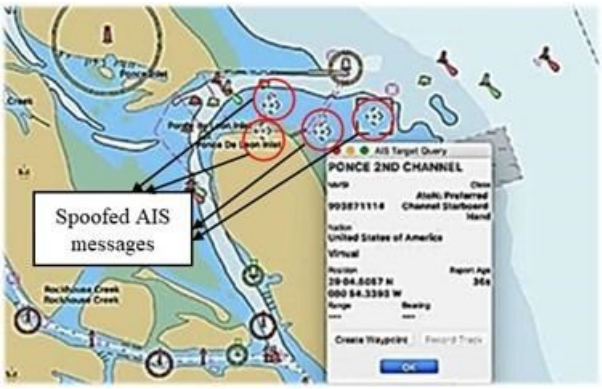

Fig. 3 Real AtoN and fake virtual AIS AtoNs (adapted from [5;11]).

For this reason, it is always recommendable to double-check the accurate electronic chart depths in narrow waterways, as well as real AtoNs like green and red buoys in this case, which clearly indicate the north part of the inlet as a navigable and safe one. This case was recorded in the Ponce de Leon Inlet on the east coast of Florida.

Both GPS and AIS are very advanced, sophisticated technologies, but extremely vulnerable to cyber-attacks. In fact, these powerful systems can be corrupted by various adversaries in various ways, using low technology, so it is necessary to work on the development of protection mechanisms or to find alternative solutions. The attempts to develop a navigation system onboard the autonomous research vessel, which can function independently of GPS and AIS, is one of the important solutions that is discussed below in this study.

2.3 Alteration to alternative navigation

In a case of cyber-attack to the satellite receiver, the ship can be switched to the alternative navigation means, such as ship's chronometer, compass, spped log, relative wind detector, Inertial Navigation System (INS) or other local sensors. For example the inertial navigation is based on a gyroscope and accelometers that can be used to integrate the path travelled by the ship over a given period. Through sensors' data fusion, ship's engine combustion and propulsion parameters can also be used to implicitly determine the ship's position, in addition to gyroscopes and speedometers. The INS is usually combined with a Kalman filter, which compares a mathematical model of the ship's behaviour in certain environmental conditions with the data from the sensors and estimates the error, i.e. corrections, which are sent back to the inertial system to improve its accuracy. The system requires the last accurately recorded position of the ship. It should also be remembered that a ship is subject to natural disturbances as wind, current and waves. Exact modeling of ship needs to take into account six degrees of freedom: yaw, sway, heave, surge, pitch, and roll, which makes modeling a challenging task.

The dynamic positioning system onboard of a ship relies on a mathematical model of the vessel and available info of local sensors. To reduce the influence of measurement errors the Kalman filter methodology may be applied that use linear theory to describe non-linear ship movement.

Our Tallinn University of Technology team is working to develop and improve the mathematical model of an experimental autonomous vessel, including local navigation controller, which may operate completely independently of the USA's GPS, or any other GNSS. Within the context, it is to be noted that besides the INS and other reliable local ship sensors, the satellite navigation can be complemented some terrestrial and astronomical navigation systems that operate independently of GNSS. For example, referential objects on land and at sea can be useful for position estimation when the vessel is relatively close to the coast or in a sailing zone of high traffic density. If the ship is offshore, at the vast sea, a nautical almanac and (digital) sextant can help determine the ship's position relative to the stars. Anyway, an important part of non-GNSS navigation is the mathematical model of the ship that will be discussed below in the present study.

3 MODEL OF THE EXAMPLE AUTONOMOUS CATAMARAN VESSEL

3.1 Example vessel

An example autonomous surface vessel for modeling studies of the present work is a catamaran "Nymo" developed in Tallinn University of Technology and dedicated for environment monitoring and cargo

transportation services [3;4], see Fig. 4.

Fig. 4 Autonomous catamaran "Nymo" developed in Tallinn University of Technology [3]. The 2.5 m long vessel is of 200 kg weight class with maximal cargo limit of 100 kg and service distance of 50 km.

3.2 Definition of modeling variables

The ship model of the present study is largely based on previous work [4], where a simplified but realistic three-degree-of-freedom (3-DOF) hydromechanical model was defined for the ASV "Nymo". Definition of main geometrical and coordinate system parameters of ship modeling task is explained by Fig. 5 below. This catamaran vessel has two hulls with separate propellers, which can produce different thrust forces F_l and F_r for the port (left) and starboard (right) hulls respectively. Fig. 5 shows the main system variable definitions where the heading angle φ represents the orientation of the vessel's body-fixed frame relative to the North-East-Down (NED) frame. Halfwidth d is the separation of side hull centerlines from ASV centerline.

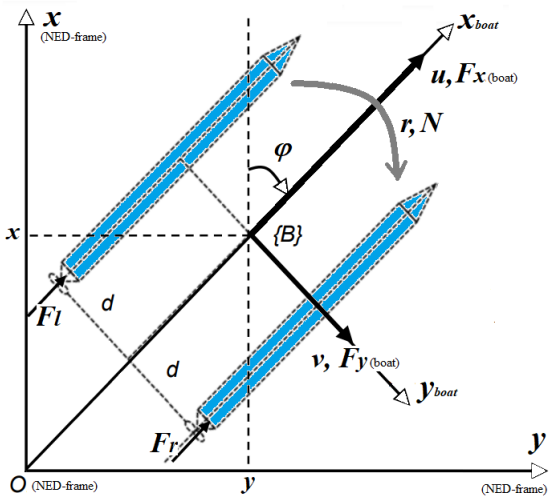

Fig. 5 Definition of variables of the 3-DOF planar model of a catamaran ASV [4]. The coordinates x and y and heading angle $\prod$ as well the rotational speed r are defined in Earth fixed North-East-Down (NED) frame. The longitudinal and lateral speeds u,v and forces F_x, F_y are defined in boat fixed inertial system.

The steering of the catamaran is accomplished by differential thrust of two propeller engines. If the thrust forces F_l and F_r are not equal, it will create the turning moment N and change of heading angle φ.

3.3 The main equations of kinematics and dynamics

The transformation of boat-frame speeds to global NED-frame speeds (the kinematics) for the considered 3-DOF task can be performed by the following matrix transform [4]

$$[\dot{x}\ \dot{y}\ \dot{\varphi}\ ] = [cos\ cos\ \varphi \quad -sin\ sin\ \varphi \quad 0 \quad sin\ sin\ \varphi \quad cos\ cos\ \varphi \quad 0\ 0\ 0\ 1\ ][u\ v\ r\ ], \tag{1}$$

where x, y and φ denote the coordinates of the center of mass and the heading angle of the ASV in the global Earth-fixed frame, and u, v, r are the velocities of surge, sway and yaw in boat-fixed local inertial system (see Fig. 5).

In order to obtain from the speeds the coordinates and heading angle, the transformation (1) must be completed with the following integration rules:

$$x(\tau) = \int_0^\tau \dot{x}(t)dt, \qquad y(\tau) = \int_0^\tau \dot{y}(t)dt, \quad \varphi(\tau) = \int_0^\tau \dot{\varphi}(t)dt \tag{2}$$

with initial state is, e. g. $x(0) = 0,\ y(0) = 0,\ \varphi(0) = /2$ (standing ASV facing East direction).

The dynamical 3-DOF hydromechanical model of catamaran can be described by the following system of equations [4;12]

$$m\dot{u} + m_{11}\dot{u} = F_x - mvr - d_{11}u\ , \tag{3a}$$
$$m\dot{v} + m_{22}\dot{v} = F_y + mur - d_{22}v\ , \tag{3b}$$
$$I_{zz}\dot{r} + m_{66}\dot{r} = N - d_{33}\,r \tag{3c}$$

where m is the catamaran mass and m_{11}, m_{22} are the added masses due to water; I_{zz} is the moment of inertia of turning catamaran around z axis and m_{66} is added rotational inertia term due to water; $d_{11},\ d_{22}, d_{33}$ are the coefficients of longitudinal, lateral and rotational hydrodynamic resistance; F_x, F_y are the external forces in longitudinal x and lateral y directions in boat-fixed frame and N is external rotational moment. Note that here water resistances are approximated by linear terms only due to lack of exact experimental results for all range of velocities. The next step towards increasing the accuracy of model for a wider range of velocities would be inclusion of quadratic water resistance terms [13].

The forces and rotational moment caused by the thrust propellers in (3) can be calculated as [13;14]

$$F_x = (F_r + F_l) + F_{wx}\ , \tag{4a}$$
$$F_y = F_{wy}\ , \tag{4b}$$
$$N = (F_l - F_r)d \tag{4c}$$

where definition of variables is explained by Fig. 5 except longitudinal and lateral wind forces F_{wx}, F_{wy} that reprecent an important environment effect introduced in this study compared to the initial work [4]. In formulation of equation (5d) is assumed the negligible rotational influence of wind. Based on [13], here are neglected thrust correction factors (see [4]). Equation (4b) assumes negligible lateral forces F_y due to propellers.

3.4 Sub-model of propeller forces

Propeller's thrusts F_r and F_l in (4) can be calculated by the following quadratic-quartic rules [13;15]:

$$F_l = k_{tl}(J_{pl})\rho_w n_l^2 d_{pl}^4\ , \tag{5a}$$
$$F_r = k_{tr}(J_{pr})\rho_w n_r^2 d_{pr}^4 \tag{5b}$$

where k_{tl} and k_{tr} are the left and right propeller thrust coefficients and J_{pl}, J_{pr} the advance speed coefficients; ρ_w is the seawater density; n_l and n_r are the propeller revolution speeds and d_{pl}, d_{pr} are the diameters of the left and right propellers, respectively. Model (5) can be refined by adding a cubic term to the dependence on propeller diameter [13] and by replacing quadratic n^2 terms with more correct $n|n|$ that acount for possibility of reversing the rotation direction.

As shown in [4], the model (5) may be simplified by introducing a dimensionless coefficient a_p similar for both propellers

$$F_{l,r} = a_p \rho_w n_{r,l}^2 d_p^4\ . \tag{6}$$

3.5 Sub-model of wind forces

In order to model the disturbances caused by natural environment, a model of wind forces acting on side surface and front surface of ASV is introduced here. The general model of wind force including dependence on 4 angles: wind direction γ_w, ship heading angle φ, angle of ship starboard normal $\varphi + \frac{\pi}{2}$, and sail angle in respect of ship body δ_s was introduced in our previous study [16]. Definition of those angles and the relevant 4 direction vectors is explained by Fig. 6 below.

In present case the imaginary sails are the ASV side surface with effective area S_{side} (sail angle $\delta_s = 0$) and ASV rear surface with effective area S_{rear} (sail angle $\delta_s = \pi/2$). The calculation of longitudinal and lateral wind forces F_{wx}, F_{wy} (see Fig. 5 and equations (4a) and (4b)) may be accomplished on the basis of the following direction vectors:

- Wind direction unit vector $\underline{w} = (cos\ cos\ (\gamma_w), sin\ sin\ (\gamma_w))$;
- Boat direction unit vector $\underline{b} = (cos\ cos\ (\varphi), sin\ sin\ (\varphi))$;
- Starboard normal direction unit vector $\underline{r} = \left(cos\ cos\ (\varphi + \frac{\pi}{2}), sin\ sin\ (\varphi + \frac{\pi}{2})\right)$;
- Sail normal direction unit vector in case of side surface $\underline{s} = \underline{r}$;
- Sail normal direction unit vector in case of rear/front surface $\underline{s} = \underline{b}$.

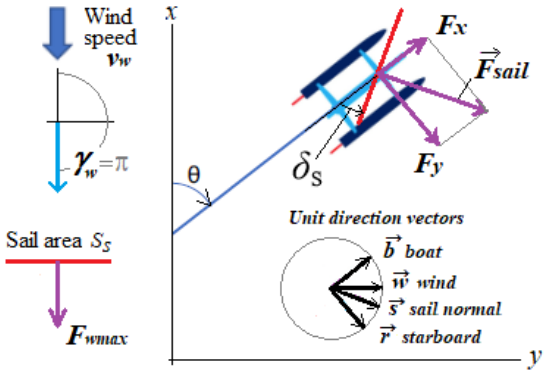

Fig. 6 Definition main angles and direction vectors of wind force calculation subtask [16].

The maximal force for wind facing the planar surface may be calculated by the following formula [16]

$$F_{wmax} = \rho S_{sail} \frac{v_w^2}{2}. \tag{7}$$

where ρ is the density of air, S_{sail} is the effective sail area (S_{side} for side surface and S_{rear} for rear surface) and surface v_w is the wind speed. With abovementioned definitions the calculation of wind force components for both surfaces may be accomplished by the following vector calculus formulas:

$$\underline{F_{sail}} = F_{wmax}(\underline{w} \cdot \underline{s})\underline{s}, \tag{8a}$$

$$F_{wx} = (\underline{F_{sail}} \cdot \underline{b}), \tag{8b}$$

$$F_{wy} = (\underline{F_{sail}} \cdot \underline{r}). \tag{8c}$$

3.6 Summary of ASV model parameters

The weight, distance between hull centers, propeller diameter and main size parameters l_x, l_y, l_d denoting the length, width and draught of ASV "Nymo" have the following values [3]:

$$m = 225\ kg,\ \ d = 0.405\ m,\ d_p = 0.18\ m, l_x = 2.56\ m,\ l_y = 1.08\ m,\ \ l_d = 0.36\ m\ .$$

Inertia and water resistance parameters of hydromechanical model (3), evaluated in previous study [4], have the following values:

$$I_{zz} = 144.75\ kg,\ \ m_{11} = 15.82\ kg\ ,\ \ m_{22} = 118.36\ kg,\ \ \ \ m_{66} = 31.36\ kg\ ,$$

$$d_{11} = 171.2\ \frac{kg}{s},\ \ \ \ d_{22} = 2d_{11},\ d_{33} = 557\ kg\ m^2/s\ .$$

Summary parameter of propeller efficiency (6) and the water density have the values [4]:

$a_p = 0.2205, \quad \rho_w = 1000\,\frac{kg}{m^3}$.

Model adjustment point for direct movement of catamaran ASV at maximal engine power [4]:

$$u = u_* = 2.57\,\frac{m}{s,} \quad n_l = n_r = n_* = 1850\,min^{-1}, \quad F_l = F_r = F_* = 220\,N\,. \tag{9}$$

For the calculations with wind force model (8) the following values for air density and effective side and rear surface areas are used:

$$\rho = 1.2928\frac{kg}{m^3}, \;\; S_{side} = 1\,m^2, \qquad S_{rear} = 0.5\,m^2.$$

4 CONTROL SYSTEM

Although in present example modeling study we have assumed linear approximation for water resistance effects in (3), the overall model (1)-(8) is still essentially nonlinear if considering dependence of 3-component output vector (x, y, φ) on propeller rotation input vector (n_l, n_r). Because of the nonlinearity of task, it is difficult to define a universal controller that satisfies all goals under all conditions.

However, the simple form of 2-component input vector offers possibility for reduction of the overall variety of control task. Actually, considering the realistic situation of catamaran navigation where the typical movement takes place on a direct course in the desired direction, the input could be reformulated to a vector, containing the difference of two propeller rotation speeds $n_{lr} = n_l - n_r$ and the maximal rotation speed of two propellers $n_{max} = max\,(n_l, n_r)$. At that, in order to minimize the influence of natural disturbances and to accomplish the patrol missions in reasonably short time, it is reasonable to fix the rotation speed of the fastest rotating propeller at relatively high level, e.g. at 90% of capability of engines stated above by adjusting condition (9), i.e. $n_{max} = 0.9n_* = 1665\,min^{-1}$. If switching to the analysis of the output vector (x, y, φ) of control task, the most important control parameter is the heading angle φ that states the desired course, and, if considering the threat of cyber attacks, is one of the least endangered parameter as its measuring is based on local onboard compasses.

Considering this, in order to further reduce the variety the control tasks, we have below simulated the tasks where output goal is the desired heading angle φ_d (either fixed or slightly corrected during the travel) and the controlled input parameter is the difference of rotations speeds of the two propellers $n_{lr} = n_l - n_r$ at fixed rotation speed of fastest rotating propeller $n_{max} = 1665\,min^{-1}$. In conventional Proportional-Integral-Derivative (PID) controller approach the control equation may be stated in the following form:

$$n_{lr}(t) = K_p e(t) + K_i \int_0^t e(\tau)d\tau + K_d\,\frac{de(t)}{dt} \tag{10}$$

where $e(t) = \varphi_d - \varphi(t)$ is the control error, i.e., the difference between the desired reference φ_d and the measurement $\varphi(t)$. Coefficients K_p, K_i, K_d specify proportional, integral and derivative terms of regulation, respectively. If the control error is measured in radians and the rotation speed in units s^{-1} then the dimensions of coefficients K_p, K_i, K_d are $s^{-1}, \; 1, and \; s$, respectively.

The block scheme of present control task with a PID controller in Simulink/MATLAB environment is illustrated by Fig. 7 below.

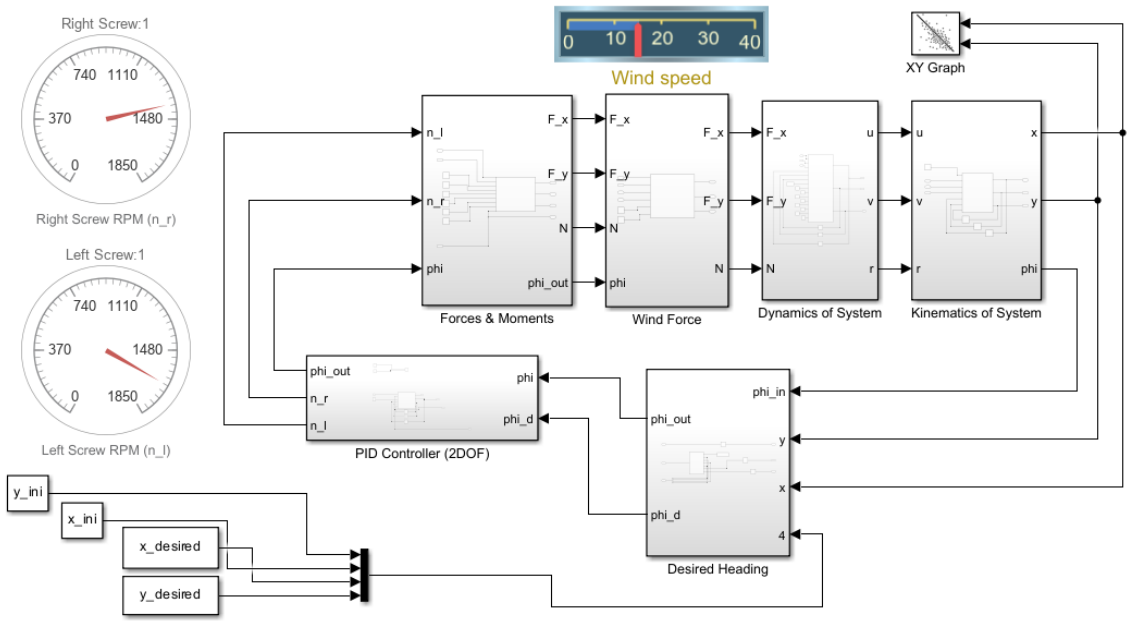

Fig. 7 Block scheme of modeling of catamaran ASV control task in Simulink/MATLAB environment.

5 SIMULATION RESULTS

5.1 Adjustment the PID-controller by the full turn task

Let us first consider the full turn 360 degrees task at zero wind to test modeling methodology and to estimate the appropriate control coefficients for PID controller equation (10). Full turn task from initial state $x = 0; y = 0;\ \varphi(0) = 90^0$ may be specified by assigning value $\varphi_d = 450^0$ for desired final angle. In the simulations, only positive values of the rotational speeds of propulsion propellers were allowed. The most characteristic input and output values and resulting trajectories for the full turn task are presented in Figs. 8 an 9 below.

As illustrated by Fig. 8, during the first turning phase of turn, the left thrust propeller maintained the limit rotation speed $n_l = n_{max} = 1665\ min^{-1}$ while the right propeller stayed at zero speed. At some time instant between 25 and 50 s that depended on proportional coefficient of controller K_p, the right propeller was turned on and the desired course was established less (smaller K_p values) or more abruptly (higher K_p values). Simulations demonstrated that the reasonable K_p values could lie between 70 and 100. Values over 200 started to cause the undesirable overshoot effect (see Figs. 8 and 9). The simulations did not show any positive effect from the integral and derivative control terms and their values are set to zero throughout the following study. Unless otherwise noted, the calculations below use a fixed value of 70 for K_p.

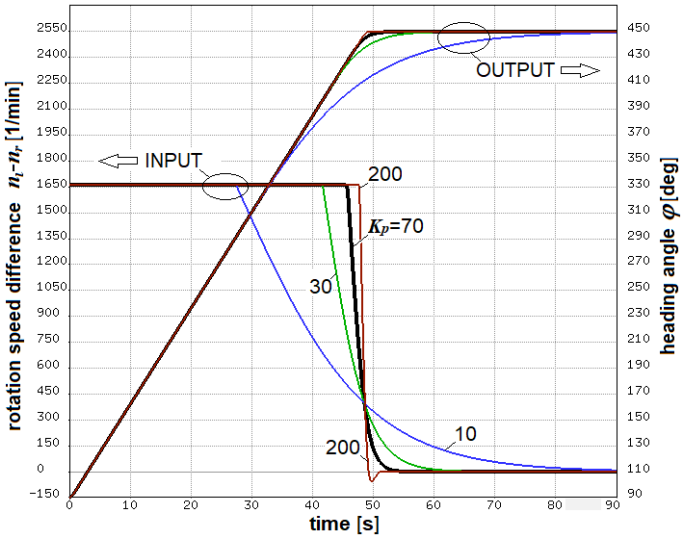

Fig. 8 Input and output of full turn test task, influence of different K_p values compared.

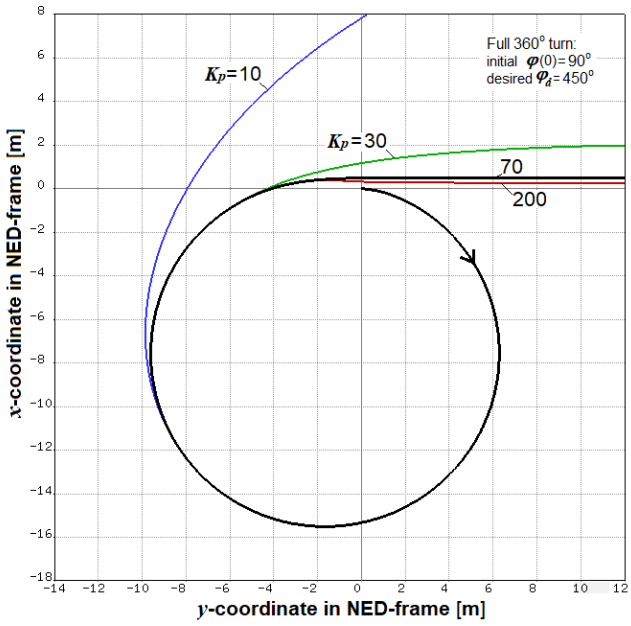

Fig. 9 Trajectories of full turn test task (zero wind), influence of different K_p values compared.

A new positive additional moment compared to the previous study [4] is that the definition of the input quantity as the difference between the rotation speeds of the two propellers eliminated the residual difference problem and the need for an integral component in the control scheme.

5.2 Simulation of 1 km example course at different wind conditions

This section deals with a realistic patrol mission task where the destination point is more than one kilometer away and the direct course is disturbed by a crosswind. Here is tested the recalculation of desired heading angle on the basis of simulated current coordinates (x, y) that are assumed to be independent of GNSS. In addition, the effect of the wind is tested, which blows from the north towards south $(\gamma_w = 180°)$ and is roughly perpendicular to the direction of the ship's movement for the most part of the journey. It can be assumed that if

the ship and wind models are accurate, then in the simulation the ship should reach the target, provided that the force of the wind does not exceed the power of the ship's engines.

Similar to the previous section, it is assumed that the ASV is initially standing at the origin of the NED-frame coordinates (0,0) and the heading angle is directed to the east ($\varphi(0) = 90^0$) before starting the initial left turn towards the destination point (100,-1000) located in the west direction (see Fig. 10 below). In addition, the secondary mission task set in the simulation conditions is that after reaching the initial destination point, the ASV will continue monitoring the sea area on a zig-zag course towards the west.

Simulated trajectories, compared in Fig. 10 demonstrate the capability of computer-aided control methodology to compensate the natural disturbance provided that the mathematical models of ASV and wind are accurate and the thrust force of propellers exceeds the wind force. It should be mentioned that in practical applications the deviation from the desired (straight) course should stay within the reasonable limits, e.g. 50 m. If fulfilling this additional requirement is important, in simulation task the auxiliary waypoints can be added between the origin and the main destination point. The wind dependences of the overall characteristics of the example trip are analysed in Table 1 and in Fig. 11 below.

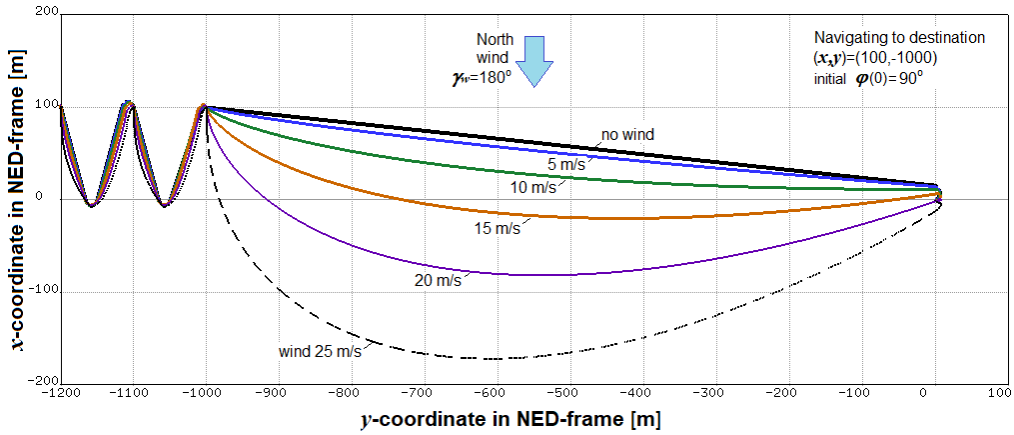

Fig. 10 Trajectories of 1 km course to destination point (100,-1000) at different speeds of disturbing north wind. After reaching the primary destination point, the ASV switches to a zig-zag course for area monitoring.

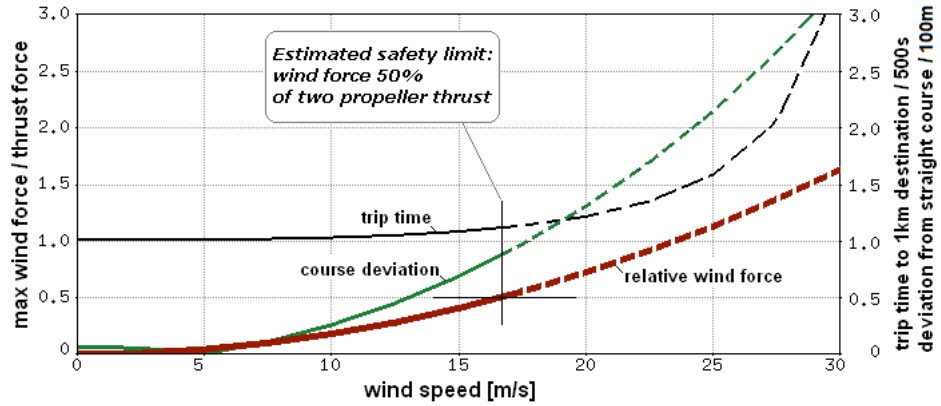

Fig. 11 Wind speed dependences of main summary parameters of course task in Fig. 10.

Speed of wind, m/s	Time to reach the destination point (100,-1000), s	Mid-trip deviation from straight line course, m	Ratio of maximal experienced wind force to thrust of two propellers, %
0	505.7	7.8	0
5	507.6	0.65	4.5
7.5	510.8	11.2	10.2

10	516.5	26.0	18.2
12.5	526.6	45.2	28.3
15	542.9	68.9	40.8
17.5	568.7	97.4	55.5
20	609.5	130.8	72.5
22.5	676.6	169.8	91.8
25	794.2	214.8	113.0
27.5	1028.1	266.8	137.2
30	1648.5	326.8	163.2

Table 1 Summary parameters of 1 km trip task of Fig. 10 in case of different north wind speed.

The results presented in Figures 10 and 11 and Table 1 show that the ASV can reach the destination even in the situation where the wind force acting on the side of the ASV exceeds the total thrust of the propellers. This can happen only due to the fact that in the last part of the journey the ship moves directly north, in which case the wind acts on twice the smaller front surface of the ship. For safe practical navigation, it is reasonable to limit the permissible wind force to some smaller percentage of the thrust of the propeller, e.g. 50% as shown in Fig. 11. If this restriction is applied, it is also possible to keep the side deviation within acceptable range as is shown in the Fig. 11.

In conclusion, the simulation example presented here shows that computer simulations based on mathematical models can provide both prediction of disturbances caused by environmental effects and safety conditions for the use of the actual ASV.

5.3 Estimating the influence of modeling inaccuracies

The results presented in the previous section showed that with perfectly accurate models for the ship and the environment, accurate control of the ship navigation to the desired end point is possible. In real-life tasks, models always have some inaccuracy, so reaching the desired target cannot be perfectly accurate. To investigate these inaccuracies, a dual modeling methodology can be used, in which the exact problem is first solved, and then the coordinates, velocities and control signals obtained from the exact problem are used in the case of inaccurate models. Figure 12 below illustrates the results of such error simulations for the already previewed 1 km journey, where it is assumed that the wind force model has a 10 to 20 percent inaccuracy, for example, because the effective sail areas are estimated somewhat inaccurately. The example case of a strong crosswind of 15 m/s analyzed in Figure 12 shows that a 10 percent wind model error may result in a relatively small deviation of 23 m over a one-kilometer course if model-based ship control would be applied.

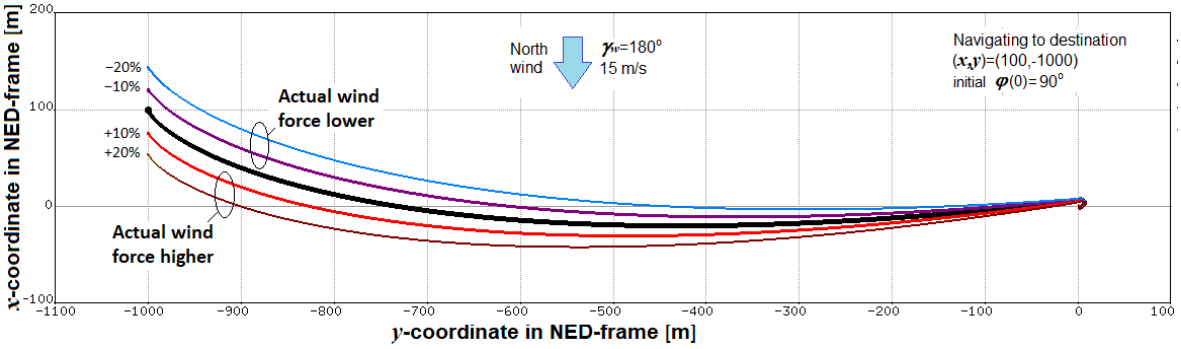

Fig. 12 Simulation of trajectory deviations due to wind model inaccuracies for 1 km course test task to destination point (100,-1000) for a strong 15 m/s north wind situation.

6 CONCLUSIONS

Modern electronic navigation systems were developed when the commercial use of the Internet was in its infancy. As a result, the threat of cyber-attacks was reduced. Today, however, we have a situation where the number of cyber-attacks in the maritime sector has almost doubled in the last five years. In maritime navigation, the most vulnerable devices to cyber-attacks are GPS and AIS. The paper gives two examples that illustrate the

dangers such attacks can pose to safe navigation, i.e. the protection of human lives, ships, cargo and the marine ecosystem. In order to respond to cyber-attacks on the satellite navigation system, an alternative solution is proposed in the paper. Namely, the mathematical model of the dynamics and kinematics of the ASV "Nymo" developed at the Tallinn University of Technology for research and experimental purposes was demonstrated. The influence of the wind on the behaviour of the ASV was analysed, as well as the parameters of the PID controller, which task is to keep the ship on the set course. The results of the simulations in Simulink/MATLAB show a high degree of accuracy of the mathematical model, as well as the appropriate response of the control system to environmental disturbances caused by wind in this specific case. It is clear that any model and any research of this kind has certain limitations. Therefore, in future research we will include currents and heavy precipitation as additional disturbance factors. It should also be emphasised that this type of ship movement control depends on the ship model, whereas the satellite navigation system determines the position and depth under the keel independently of the ship model. This reflects the universality and elegance of global satellite positioning and navigation, but if this system fails in the midst of a cyber-attack, it is necessary to have an alternative solution. A very effective one, independent on satellite positioning system, is presented in this paper.

7 REFERENCES

[1] Bauk, S. Performances of some autonomous assets in maritime missions. *TransNav, the International Journal on Marine Navigation and Safety of Sea Transportation* [online]. 2021, vol. 14, no. 4, p. 875-881. [Accessed: 30 April 2024]. eISSN: 2083-6481. Available at: http://doi:10.12716/1001.14.04.12

[2] Bauk, S.; Kapidani, N.; Lukšić, Ž.; Rodrigues, F.; Sousa, L. Autonomous marine vehicles in sea surveillance as one of the COMPASS2020 project concerns. *Journal of Physics: conference series* [online]. October 2019, vol. 1357, 012045. [Accessed: 30 April 2024]. eISSN: 1742-6596. Available at: http://doi:10.1088/1742-6596/1357/1/012045

[3] *MindChip [a spin-off company of Tallinn University of Technology]* [online]. [Accessed: 21 February 2024]. Available at: https://mindchip.ee

[4] Astrov, I.; Udal, A.; Mõlder, H.; Jalakas, T.; Möller, T. Experimentally Adjusted modeling and simulation technique for a catamaran surface vessel. In: *Proceedings of the International Conference on Electrical, Computer and Energy Technologies (ICECET) 2022* [online]. Prague, Czech Republic, 2022. [Accessed: 30 April 2024]. Available at: doi 10.1109/ICECET55527.2022.9873069

[5] Kessler G. C.; Shepard S. D. *Maritime cybersecurity : a guide for leaders and managers*. Dartford: One Publishing, 2022. ISBN: 9798412526034

[6] Kjerstad N. *Electronic and acoustic navigation systems for maritime studies*. Ålesund : NTNU, Norwegian University of Science and Technology, 2016. ISBN: 9788292186572

[7] ADVA tackles GNSS jamming and spoofing with AI solutions. In: *GPS World* [online]. North Coast Media, 2024. [Accessed: 20 February 2024]. Available at: https://www.gpsworld.com/adva-tackles-gnss-jamming-and-spoofing-with-ai-solution/

[8] About EGNOS. In: *Egnos user support* [online]. EUSPA, ESSP, 2024. [Accessed: 17 February 2024]. Available at: https://egnos-user-support.essp-sas.eu/egnos-system/about-egnos

[9] Burgess, Matt. When a tanker vanishes, all the evidence points to Russia. In: *Wired* [online]. 21 September 2017. [Accessed: 17 February 2024]. Available at: https://www.wired.co.uk/article/black-sea-ship-hacking-russia

[10] ASGARD: the ultimate response to maritime spoofing attack. In: EUSPA. *News and events* [online]. 29 September 2023. [Accessed: 17 February 2024]. Available at: https://www.euspa.europa.eu/newsroom-events/news/asgard-ultimate-response-maritime-spoofing-attacks

[11] Kessler G.C. Protected AIS: a demonstration of capacity scheme to provide authentication and message integrity. *TransNav, the International Journal on Marine Navigation and Safety of Sea Transportation* [online]. 2020, vol. 14, no. 2, p. 279-286. [Accessed: 30 April 2024]. Available at: http://doi:10.12716/1001.14.02.02

[12] Hong, M.J. Arshad, M.R. Modeling and motion control of a riverine autonomous surface vechicle (ASV) with differential thrust. *Jurnal Teknologi* [online]. 2015, vol. 74, no. 9, p. 137-143. [Accessed: 30 April 2024]. eISSN: 2180-3722. Available at: https://doi.org/10.11113/jt.v74.4817

[13] Wirtensohn, S.; Reuter, J.; Blaich, M,; Schuster, M.; Hamburger, O. Modelling and identification of a twin hull-based autonomous surface craft. In: *2013 18th International Conference on Methods & Models in Automation & Robotics (MMAR*) [online]. Miedzyzdroje, Poland, 2013, p. 121-126. [Accessed: 30 April 2024]. Available at: doi: 10.1109/MMAR.2013.6669892

[14] Ferrari, V.; Sutulo, S.; Soares, C.G. Preliminary investigation of berthing of waterjet catamaran. In: Soares C.G.; Santos, T.A. (eds.). In: *Maritime Technology and Engineering.* London: CRC Press, 2014, p. 1105-1112, [Accessed: 30 April 2024]. eISBN: 9780429226663. Available at: https://doi.org/10.1201/b17494

[15] Pandey, J.; Hasegawa, K. Path following of underactuated catamaran surface vessel (WAM-V) using fuzzy waypoint guidance algorithm. In: Bi, Y.; Kapoor, S.; Bhatia, R. (eds). *Proceedings of SAI Intelligent Systems Conference (IntelliSys) 2016. IntelliSys 2016*. Cham: Springer, 2017. Lecture Notes in Networks and Systems, vol 16. p. 616-627. [Accessed: 30 April 2024]. eISNB: 9783319569918 Available at: https://doi.org/10.1007/978-3-319-56991-8_45

[16] Astrov, I.; Udal, A.; Mõlder, H.; Jalakas, T.; Möller, T. Wind force model and adaptive control of a catamaran model sailboat. In: *2022 8th International Conference on Automation, Robotics and Applications (ICARA).* Prague, Czech Republic, 2022, p. 202-208 [Accessed: 30 April 2024]. Available at: doi: 10.1109/ICARA55094.2022.9738524